Revista EIA

UNIVERSIDAD EIA

# Crosslinked alginate-chitosan based scaffold functionalized with VEGF-A for the beta-pancreatic cells support



Revista EIA
ISSN 1794-1237
e-ISSN 2463-0950
Año XIX/ Volumen 22/ Edición N.43
Enero - junio 2025
Reia4305 pp. 1-24

Publicación científica semestral
Universidad EIA, Envigado, Colombia

**Para citar este artículo / To reference this article /**
Betancur Rodríguez, M.; Echeverri-Cuartas, C. E.; Londoño López, M. E. y Moreno-Castellanos, N. Crosslinked Alginate-Chitosan Based Scaffold Functionalized with VEGF-A for the Beta-Pancreatic Cells Support

Revista EIA, 22(43), Reia4305 pp. 1-24.
https://doi.org/10.24050/reia.v22i43.1838

*Autor de correspondencia:*

Moreno-Castellanos, N.
Bacteriólogo
Correo electrónico:
nrmorcas@uis.edu.co

**Recibido:** 27-09-2024
**Aceptado:**10-12-2024
**Disponible online:** 01-01-2025

Manuela Betancur Rodríguez[1]
Claudia E Echeverri-Cuartas[1]
Marta E Londoño López[1]
Natalia Moreno-Castellanos[2]

1. Universidad EIA, Colombia.
2. Universidad Industrial de Santander, Colombia.

## Abstract

Diabetes has become a global public disease that affects the quality of life of people and demands high costs in health systems. Diabetes increases the blood glucose levels and induces inappropriate insulin use; current treatments are not very efficient in treating this disease. In this study, a porous alginate (Alg)/ chitosan (Ch) scaffold, cross-linked with genipin (GEN), functionalized with endothelial growth factor (VEGF-A) by carbodiimide-Ch coupling, was developed to support beta-pancreatic cells. Characterizations such as scanning electron microscopy (SEM) and, Fourier transform infrared spectroscopy (FTIR) were used to identify functional groups and observe the morphology and porosity of the scaffolds. Degradation and swelling velocity tests were performed following by biological tests such as cell viability, cell cytotoxicity and proliferation assays were measured in all the samples. The scaffolds obtained had a sponge-like structure with interconnected pores with diameters less than 25-280 µm, suitable for beta-pancreatic cells growth and islet formation. These matrices degrade are stable over time and allow cell culture while maintaining beta-cell viability and proliferation. It additionally generates protection against cell death by inducing an appropriate environment to preserve viability and also through the action of VEGF in combination with GEN induces the proliferation of beta cells. This approach allows the design of a matrix with biomimetic properties for insulin-producing cells culture and represents a significant advance in the field of medicine and life sciences.

***Keywords:*** beta-pancreatic; scaffold; insulin, diabetes, genipin; chitosan; alginate; endothelial growth factor; cells; proliferation.

# Andamio reticulado a base de alginato-quitosano funcionalizado con VEGF-A para el soporte de las células betapancreáticas

## Resumen

La diabetes se ha convertido en una enfermedad pública mundial que afecta la calidad de vida de las personas y exige altos costos en los sistemas de salud. La diabetes aumenta los niveles de glucosa en sangre e induce el uso inadecuado de insulina; los tratamientos actuales no son muy eficaces para tratar esta enfermedad. En este estudio, se desarrolló un andamio poroso de alginato (Alg)/quitosano (Ch), reticulado con genipina (GEN), funcionalizado con factor de crecimiento endotelial (VEGF-A) mediante acoplamiento carbodiimida-Ch, para soportar las células beta-pancreáticas. Se utilizaron caracterizaciones como microscopía electrónica de barrido (SEM) y espectroscopia infrarroja por transformada de Fourier (FTIR) para identificar grupos funcionales y observar la morfología y porosidad de los andamios. Se realizaron pruebas de velocidad de degradación e hinchazón y luego se realizaron pruebas biológicas como viabilidad celular, citotoxicidad celular y ensayos de proliferación en todas las muestras. Los andamios obtenidos tenían una estructura similar a una esponja con poros interconectados con diámetros entre los rangos 25-280 µm, adecuados para el crecimiento de células beta pancreáticas y la formación de islotes. Estas matrices se degradan, son estables en el tiempo y permiten el cultivo celular manteniendo la viabilidad y proliferación de las células beta. Adicionalmente, genera una protección contra la muerte celular induciendo un ambiente apropiado para preservar la viabilidad e incluso por la acción del VEGF en combinación con GEN, induce la proliferación de células beta. Este enfoque permite el diseño de una matriz con propiedades biomiméticas para el cultivo de células productoras de insulina y representa un avance significativo en el campo de la medicina y las ciencias de la vida.

***Palabras clave:*** beta-pancreatica; andamio; insulina; diabetes; genipina; quitosano; alginato; factor de crecimiento endotelial; celulas; proliferación.

## 1. Introduction

Type 1 diabetes Mellitus (DM) is characterized by high glucose plasma levels. This disorder leads over time to an insulin secretion alteration on the specialized cells of the pancreas (beta-pancreatic cells) or alterations in tissue effectors that lead to a loss of sensitivity in one or more points of the complex pathways of the hormonal action of insulin. In recent years, 11 individuals worldwide have suffered from this disease, representing an alarming increase in the incidence of diabetes (Norris *et al.*, 2020). According to estimates, 415 million adults worldwide had diabetes in 2015, and by 2040, this number will be 642 million (Maniruzzaman *et al.*, 2020). This disease is associated with severe health complications, such as visual problems, diabetic foot, kidney failure, and neuropathy, affecting the patient and generating high costs in the comprehensive social security system. In addition, the total costs related to diabetes are higher in Latin America and the Caribbean. The economic burden has been estimated at US $65,000 million per year of gross domestic product (GDP) in most countries (Adey *et al*., 2020).

Insulin dosing by exogenous routes, which is highly invasive and painful, or a complete pancreas transplant, which could present rejection, does not meet the needs of patients with diabetes or improve their quality of life (Brawerman and Thompson, 2020). Therefore, advances in alternative therapies forrestructuring and functionalizing specialized endocrine cells of the pancreas based on cellular and molecular mechanisms associated with diabetes are promising.

Cell-biomaterial interactions have emerged as a potential field to provide strategies for the immunoprotection of pancreatic islets (Hu and de Vos, 2019; Song and Roy, 2016). Primarily, matrices are used to maintain pancreatic beta cells in semi-permeable polymeric membranes with glucose-sensitive properties (Hu and de Vos, 2019; Yang *et al.*, 2021). Several studies on hydrogel platforms have been proposed for diabetic applications (Chua *et al.*, 2018). However, the use of hydrogels based on Alg and Ch blends with GEN as a crosslinker has not yet been explored for the culture of insulin-

producing cells. Alg is a biomaterial with great biocompatibility properties and low toxicity, structural similarity with life tissues of the extracellular matrix (ECM), minimization of bacterial infection at the wound site, and facilitation of healing and low cost (Dhamecha *et al.*, 2019). On the other hand, Ch is a natural polymer, too, and has good biocompatibility, controlled biodegradation, and antibacterial properties (Zhao *et al.*, 2018). Given the poor mechanical properties of Ch, covalent crosslinking with GEN was used (Kildeeva *et al.*, 2020). GEN acts specifically on the uncoupling protein 2 (UCP2)-dependent manner increasing mitochondrial membrane changes on the ATP channels that leads to the the insulin secretion into the pancreatic islets cells that reverses the high levels of plasma glucose and beta cell disfunction (Zhang *et al.*, 2006). The matrices with GEN are not cytotoxic and promote cell adhesion, proliferation, and migration, according to tests carried out by other authors on human cells and in vivo tests (Gao *et al.*, 2014). Finally, VEGF-A has been used to functionalize beta-pancreatic cell scaffolds (Lammert *et al.*, 2003) because it promotes cell survival, proliferation, differentiation, angiogenesis, and blood glucose regulation, and increases the interaction of beta-pancreatic cells with the circulatory system (Lammert *et al.*, 2003). This study aimed to evaluate a polymeric scaffold based on Alg/Ch/GEN functionalized with VEGF-A for insulin-producing cell growth and proliferation as a strategy for tissue engineering in diabetes.

## 2. Materials and Methods

### *2.1. Scaffold Preparation*

A chitosan (Ch) (medium molecular weight, Sigma Aldrich, lot # SLBG4282V) solution was prepared at 1 % w/v by dissolving it in acetic acid solution (2 %v/v). Alg (low viscosity, Sigma-Aldrich) solution 1 % w/v was prepared in deionized water. For scaffold functionalization with VEGF-A, Alg solution 1 % w/v was dissolved in 20 % citrate buffer (pH = 6) and 80% deionized water. The reaction with 1-ethyl-3-(3-(dimethylamino) propyl)- carbodiimide (EDC) and N-hydroxysuccinimide (EDC/NHS) was performed on ice for 2 h, and the Alg solution was incubated with 1 ng of VEGF-A (Sigma Aldrich)


Revista EIA https://doi.org/10.24050/reia.v22i43.1838

for 12 h at 600 rpm. Finally, a 25% w/v GEN solution (G4796, Sigma Aldrich) was prepared in 60% v/v ethanol.

The scaffold formation was mixed with Alg/Ch in a 20/80 proportion (M1), then GEN was added at 0.5% and 1% w/w without VEGF-A (M2 and M3, respectively) and GEN 0.5% or 1% w/w functionalized with VEGF-A (M4 and M5, respectively); this proportion was based on 1% total mix chitosan weight. It was homogenized by sonication for 10 min with cycles of 40 s on and 10 s off at an amplitude of 35% (Vibra Cell, Sonics). For porous formation, the samples were placed at 37 °C for 48 h, frozen at -20 ºC for 24 h, and lyophilized at -50 ºC for 24 h at 10 mTorr (Virtis, SP Scientific). Control samples were prepared with an Alg/Ch ratio 20/80 (M1), without GEN and VEGF-A. All treatments were performed in triplicates.

### *2.2. SEM Analysis*

The electron microscopy (SEM) (Phenom ProX) was used to obtain photomicrographs of scaffold surfaces at an accelerating voltage of 15 kV. The morphology and microstructure of the scaffolds were observed. To measured matrices pore size the ImageJ software was used.

### *2.3. FTIR Analysis*

Fourier-transform infrared (ATR-FTIR) spectroscopy was used to evaluate the bands of the composite scaffold using a PerkinElmer, USA with a wavenumber of 4000–650$cm^{-1}$, 25 scans per sample, and a relative pressing force of 80%.

### *2.4. Swelling of Polymeric Matrices*

The swelling ratio of each scaffold (M1-M5) was determined using rectangular pieces (approximately mm). The dry weights of the samples were measured using an electronic balance (Denver Instruments), recorded $W_0$. Samples were recovered every 24, 48, 72, 96, 120, and 144 h in phosphate-buffered saline (PBS) and the wet weight of the scaffold ($W_t$) was measured. The wet weights ($W_t$) were

not measured until the weight displayed on the electronic balance no longer changed (Hsieh *et al.*, 2007). At least three samples were measured per each time under the same conditions.

The water absorption of these samples was calculated using the Equation 1:

$$Swellingratio(\%) = \frac{W_t - W_0}{W_0} \times 100 \qquad (1)$$

### *2.5. In vitro Degradation*

Scaffold biodegradability was assessed by monitoring weight loss over four weeks. Initially, three samples of the scaffold were cut into rectangles of the same size (approximately 6 x 4 mm) and analyzed for 28 days. The dry weights ($W_i$) of the samples were measured whashed with PBS and incubated at 37 °C. After incubation for 28 days, the scaffolds were removed from the medium, dried, and their final weight ($W_f$) was recorded.

The percentage of degradation (D) of these samples was calculated using the Equation 2:

$$Degradation(\%) = \frac{W_i - W_f}{W_i} \times 100 \qquad (2)$$

### *2.6. Cell Culture*

BRIN-BD11 cells ich is a beta-pancreatic cell line (Cell Bank, Coleraine, Northern Ireland, U.K) were ultured at a $4\times10^4$ cells/cm$^2$ cell density, pancreatic cells were cultured as was described before (Sánchez-Cardona *et al.*, 2021). Briefly, cells were incubated at 37 °C under 5% $CO_2$ in Dulbecco's Modified Eagle Medium: Nutrient Mixture F-12 (DMEM-F12 -GlutaMAX-I) (Gibco, New York, NY, USA) supplemented with 10%, fetal calf serum, 1% (v/v) antibiotic/ antimycotic solution (Gibco, New York, NY, USA).

The biomaterials samples were sterilized with UV-C irradiation for 20 min, washed with PBS three times, and placed in a 24 well-plate. Then, cells were dispersed with trypsin (w/v) and cultured on the scaffolds at $4\times10^4$ cells/cm$^2$, and incubated for three days at 37ºC/5% $CO_2$.


Revista EIA https://doi.org/10.24050/reia.v22i43.1838

### *2.7. Cell viability Assay*

To evaluate the effect of the scaffolds on beta pancreatic cell viability, the MTT (3-(4,5-Dimethylthiazol-2-yl)-2,5-diphenyltetrazolium bromide) assay was measured as was described before (Anjani *et al.*, 2022; Sánchez-Cardona *et al.*, 2021). Briefly, the MTT solution was added to the culture and after 8 hr of incubation and the crystals were formed, the (dimethyl sulfoxide) (99.7%, Sigma Aldrich, St. Louis, MO, USA) was added to dissolve the formazan crystals, the absorbance was read at 570 nm on a Synergy H1 microplate reader (Biotek, Winooski, VT, USA). The plate culture cells were used as control without any biomaterial.

### *2.8. Live and Dead Staining*

For live/dead staining, the protocol has been previously described (Anjani *et al.*, 2022). Briefly, the were washed followed by the stained with ethidium homodimer-1 (Molecular Probes, Eugene, Oregon, USA) and calcein AM and 5 $\mu g$/mL during 5 minutes. Fluorescence images were obtained using an Olympus Fluoview Confocal Microscope.

### *2.9. Lactate Dehydrogenase (LDH) Assay*

The LDH assay quantifies the cytosolic lactate dehydrogenase enzyme released in the culture medium by cells with damaged membranes. The protocol has been described before (Anjani *et al.*, 2022). Specifically, washed cell suspension was incubated with 2% Triton X-100 (v/v) during 30 min at 37°C. Then, lysed cell solution from each well was incubated again at 37°C for 30min. The final solution was placed to a 96-well plate. The absorbance was read at 490 nm with 620 nm as the reference wavelength. The percentage of cell death was determined by re-leasing LDH from live samples normalized to the positive control samples (or lysis buffer treated).

### *2.10. Cell Proliferation*

Proliferation was measured evaluating the number of DNA copies formed by each cell cycle as was described before(Anjani *et al.*, 2022). The amount of DNA in the cells attached to the biomaterials was

determined using Quant-iT™ PicoGreen® dsDNA Reagent and Kits (Molecular Probes, Life Technologies Corp.) as the manufacturer's instructions. Specifically, The samples were washed and mixed with lysis buffer. To release the DNA samples were vortexed and homogenized during 10–15 min. The sample was incubated with DNA-binding fluorescent dye solution and the fluorescence as measured at 480 to 520 nm. Lambda DNA was used as the standard curve to calculate the amount of DNA. Samples (n=3) were prepared in triplicate.

### *2.11. Statistical Analysis*

Data are expressed as mean ± SEM. Statistical differences between mean values were analyzed using one-way ANOVA with multiple post-hoc-Turkey test. A comparison of the two variants was performed using the student's t-test. Statistical significance was set at $P<0.05$. Statistical analyses were performed using SPSS/Windows version 15.0 software (SPSS Inc. Chicago, IL, USA).

## 3. Results and Discussion

### *3.1. SEM Analysis*

The obtained scaffolds had a sponge-like structure and retained the shape and thickness of the mold. In addition, the matrixes exhibited a regular and homogeneous surface with a rough appearance. On the other hand, the scaffolds treated with GEN had a bluish coloration, characteristic of matrices crosslinked using this compound, which has been widely reported in other studies (Dimida *et al.*, 2017). Figure 1 shows the SEM micrographs obtained at 400X magnification of the cross, upper, and lower sections of each matrix, in which there are interconnected pores. Matrices containing GEN and VEGF-A had larger pores that were slightly rounder. SEM micrographs show all the walls of the samples and have small pores that allow greater communication between the cells; however, those in the presence of VEGF-A (M4 and M5) have more porous walls.

The pore sizes were calculated by analyzing the SEM micrographs of each matrix using ImageJ software. The results showed that


Revista EIA https://doi.org/10.24050/reia.v22i43.1838

approximately 90% of the matrix pores had sizes in the range of 25 – 300 μm. Structures with interconnected pores have been reported to mimic, at least to a large extent, tissues in their natural state, allowing not only a simulation of normal tissue but also nutrient and gas exchange that can greatly support cell proliferation (Shi *et al.*, 2002), and thus, contribute to enhancing the outcomes of the 3D scaffolds, especially those functionalized with VEGF-A.

The most frequent minimum pore sizes were those between 30 and 75 μm. According to Madden et al., a pore size with a minimum size of 30-40 μm maximizes vascularization and allows the infiltration of blood vessels into the scaffolds (Madden *et al.*, 2010). By promoting vascularization on scaffolds, the survival of pancreatic islets is expected to be improved by reducing cellular apoptosis caused by hypoxic conditions.

Comparing the samples by the percentage of GEN, that is, those with 0.5% with 1%, specifically, M2 (145.5 μm) vs M3 (248.0 μm) and M4 (272.9 μm) vs M5 (283.7 μm), it was found that samples what had a percentage of GEN 1% had larger pore size diameters. This could be because a low concentration of GEN generates weak chemical crosslinking between the polymers, and a network of less-structured pores is formed.

In contrast, comparing the maximum pore size of the samples with the same percentage of GEN, but with or without the presence of VEGF-A. Specifically, M2 (145.5 μm) and M3 (248.0 μm) vs M4 (272.9 μm) and M5 (283.7 μm), the VEGF-A scaffolds have larger pores. This could be due to the capacity of VEGF-A protein to modify the pore size in some biomaterials (Antonova *et al.*, 2016; Chakka *et al.*, 2021). According to the pore size, the islets of Langerhans have a radius of 50-250 μm, in which β-cells and other secretory cells are densely packed (Bertram and Pernarowski, 1998). Pores of 200 and 300 μm have been found to induce physiological cellular organization of pseudo-islet β cells (Ichihara *et al.*, 2016). Therefore, in terms of the ranges necessary for the culture of β-pancreatic cells and islets of Langerhans, samples M1, M3, M4, and M5 have more suitable pore diameters for β-pancreatic cell culture and the pseudo-islets for β-cells formation.

***Figure 1.*** *Representative SEM micrographs view of the cross (left), upper(middle), and lower (right) sections of the developed M1 to M5 scaffolds.*

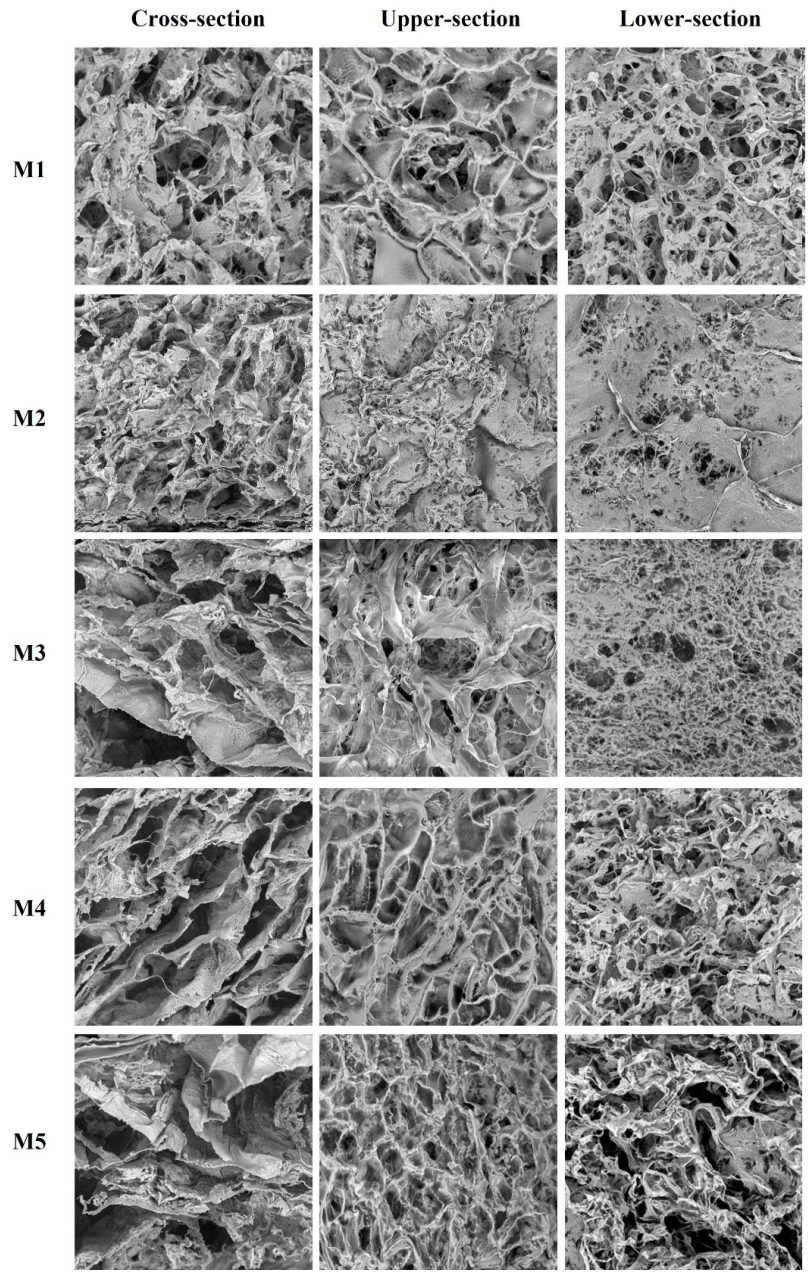


### *3.2. FTIR Analysis*

The infrared spectra of all the samples are presented in Figure 2. In all cases, a band width at 3411 $cm^{-1}$ associated with the vibrational stretching of the -OH groups of both chitosan and alginate, is evident. In this same region, the vibration associated


Revista EIA https://doi.org/10.24050/reia.v22i43.1838

with stretching the -$NH_2$ groups of chitosan is overlayed (Garnica-Palafox *et al.*, 2020; Tavares *et al.*, 2020). Additionally, in all samples, the absorption bands around 2929 $cm^{-1}$ and 2858 $cm^{-1}$ can be attributed to symmetric and asymmetric stretching of the C–H bond, respectively (Queiroz *et al.*, 2015).

Around 1633 $cm^{-1}$, there is a signal attributed to the vibration of the C=O bond of the acetylated units of chitosan (groups –C(O) $NH_2$, amide I); at 1545 $cm^{-1}$ there is a signal associated with the bending vibrations N–H bond of amide II of chitosan (Garnica-Palafox *et al.*, 2020). The signal at 1407 $cm^{-1}$, also present in all samples, is associated with $CH_2$-CH and CH-OH bending vibrations (Garnica-Palafox *et al.*, 2020). Finally, at 1151 $cm^{-1}$, there is a signal associated with the asymmetric stretching vibrations of the C–O–C bond, and at 1069 $cm^{-1}$ and 1031 $cm^{-1}$, there are present the stretching vibrations of the C-O and C-N bonds, respectively (Klein *et al.*, 2016; Tavares *et al.*, 2020). The C-O bonds occur for both chitosan and alginate, but the C-N bond is characteristic only of chitosan. Due to the above, these signals are present in all the samples analyzed.

***Figure 2.*** *FTIR Spectroscopy analysis of M1 to M5 scaffolds.*

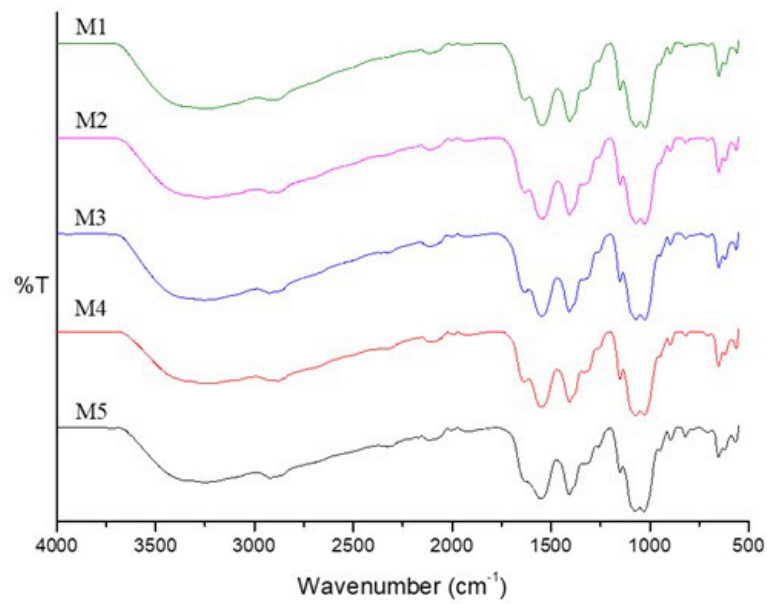

Concerning the crosslinking of GEN with chitosan, the reaction through a nucleophilic attack of the amino group of Ch on the olefinic carbon of GEN implies the opening of the dihydropyran ring and the formation of a tertiary amine, with GEN attached to a glucosamine unit of Ch as a final product. The slowest reaction posterior between the amino group of chitosan and the ester group of GEN forms an amide bond (Klein *et al.*, 2016). Therefore, the main chemical differences observed by infrared spectroscopy occur between 3500 $cm^{-1}$ and 3000 $cm^{-1}$ and between 1600 $cm^{-1}$ and 1500 $cm^{-1}$ (Garnica-Palafox *et al.*, 2020). Following the above, for the samples crosslinked with GEN (M2, M3, M4, and M5) and modified with the growth factor (M4 and M5), a comparison was made of the intensity of the absorbance peak in the region of 3411 $cm^{-1}$ and 1545 $cm^{-1}$. Figure 3 shows a decrease in the intensity of the signals in the two previously mentioned regions due to the consumption of ami Figure 2 no and hydroxyl groups during the crosslinking reaction (Garnica-Palafox *et al.*, 2020). The decrease is more significant for the samples modified with the growth factor because the modification reaction with carbodiimide also consumes amino groups from chitosan.

***Figure 3.*** *FTIR Spectroscopy analysis in absorbance of M1 to M5 scaffolds. (a) Whole spectrum and (b) Region 1800 to 850 cm-1.*

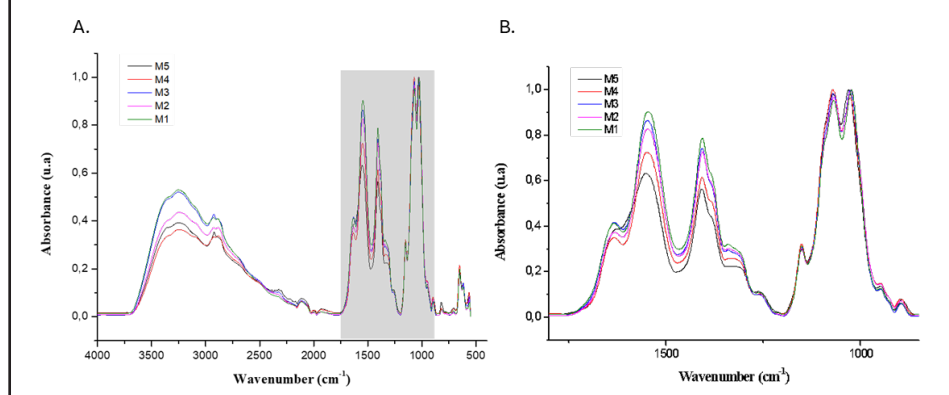


After normalizing all the spectra, a quantitative analysis was performed through the ratio of the intensities of the signal at 1545 $cm^{-1}$ and the signal at 1151 $cm^{-1}$ (Table 1) since the first band (1545 $cm^{-1}$) decreases with the modification and


Revista EIA https://doi.org/10.24050/reia.v22i43.1838

crosslinking, and the second (1151cm$^{-1}$), which corresponds to the C–O–C bond, does not change with the reactions mentioned above. The results of this intensity ratio indicate that samples M2 and M3, compared to M1, have a difference in the intensity ratio of approximately 0.1, indicating that the intensity of the signal decreases at 1545 cm$^{-1}$ due to the crosslinking reaction with GEN that leads to the formation of secondary amides due to the reaction between the ester and hydroxyl groups of GEN and the amino groups of chitosan (Garnica-Palafox *et al.*, 2020).

When comparing samples M4 and M5, which in addition to being cross-linked, were also modified with the growth factor, the difference in the ratio of intensities concerning M1 is approximately 0.7, thus indicating that there is a greater consumption of amino groups due to cross-linking and modification processes. These results suggest a successful modification and cross-linking in the samples.

***Table 1.*** *Intensity ratio for all samples and intensity differences for the samples crosslinked and modified with the growth factor.*

| Sample | Intensity Ratio (Intensity 1545/ Intensity 1151) [a)] | Intensity differences [b)] |
|---|---|---|
| M1 | 2,952 | --- |
| M2 | 2,777 | 0,175 |
| M3 | 2,846 | 0,106 |
| M4 | 2,308 | 0,644 |
| M5 | 2,180 | 0,772 |

a)The intensity ratio was calculated as the division between the intensity of the signal at 1545cm $^{-1}$ and the intensity of the signal at 1151 cm$^{-1}$. Intensities were calculated using the spectrum in absorbance units and using Origin® software; b) The difference in intensity was calculated using M1 as a reference, which was the sample without crosslinking and without a growth factor. Intensity ratio values were used for each of the samples.

### *3.3. Swelling of Polymeric Matrices*

In cell culture, swelling of scaffolds is relevant, mainly because it favors the transport of fluids, metabolites and nutrients within the scaffold, improving the surrounding environment for cell support and survival. Swelling also modifies the pore size increasing the internal surface of the scaffolds for better adherence to the developed matrices (Maji *et al.*, 2016). Figure 4 shows the swelling percentage of all treatments (M1 to M5) during 144 h. Samples reached equilibrium after 42 h in PBS at 37 °C, which could be explained by their being porous, allowing fluid to pass through for a given time until the porous medium becomes impermeable (Hommel *et al.*, 2018). Radius is a significant factor controlling the permeability of porous structures (Nishiyama and Yokoyama, 2017).

***Figure 4.*** *A swelling ratio over time of M1 to M5 scaffolds.*

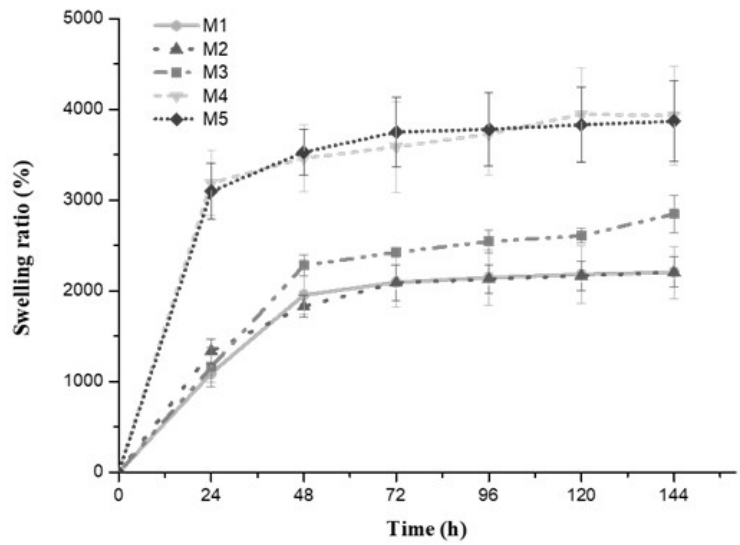


According to Figure 4, M2 was found to have a lower swelling ratio than M3. At pH 7.4 carboxyl group in alginate is ionized; therefore, M2 should swell more. Nevertheless, in the M3 sample, chitosan is more crosslinked with GEN, which could displace the electrostatic interactions between chitosan and alginate, making carboxyl groups in alginate more available to interact with water.


Revista EIA https://doi.org/10.24050/reia.v22i43.1838

Moreover, when contrasting this result with size pores, M3 had more pores, confirming a minor restriction to water uptake.

Furthermore, it was found that M2 y M3 had less swelling behaviour than M4 and M5. The last could be explained since M2, and M3 only have GEN, while M4 y M5 have GEN and VEGF-A. The VEGF-A presence could alter the hydrophilic/hydrophobic balance in the scaffold, but further analysis should be used in the future to explain the role of VEGF-A in the scaffold.

### *3.4. In vitro Degradation*

Figure 5 shows the percentage of degradation every 7 days during 4 weeks of M1 to M5 scaffolds. The graph shows that all the scaffolds presented weight loss during this time.

Comparing the samples according to the GEN percentage, scaffolds with GEN 0.5% have a higher rate of degradation (M2 = 24.3% and M4 = 43.0%) in contrast with GEN 1% samples (M3 = 19.4% and M5 = 27.5%); this could be explained because they are less crosslinked and have more mechanical weakness. In addition, the M1 sample has a low weight loss percentage (22.7%) mainly because the Alg-Ch scaffold is not crosslinked with GEN. This result could be for the Ch and Alg charges (positive and negative, respectively), during the synthesis, an electrostatic interaction occurs, which allows the scaffold to preserve its structure (Belén *et al.*, 2009).

***Figure 5.*** *Degradation total percentage of M1 to M5 scaffolds.*

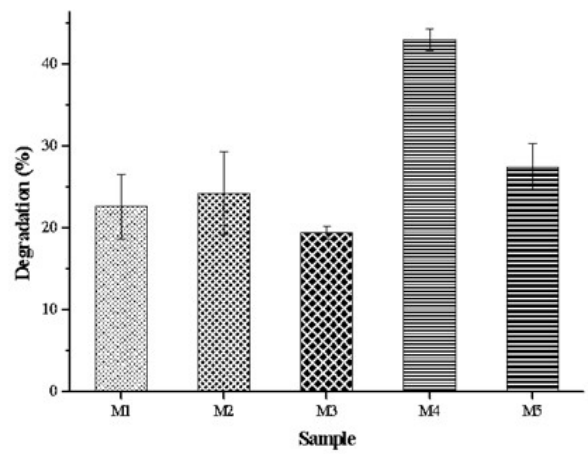

Finally, after measuring the pH of the medium every week, it presented acidification of approximately 2%, considering that the initial PBS pH was 7.41. This variation in pH may be explained because the pKa of Ch is around 5.5-6.5 and, since PBS has a pH above the pKa, electrostatic interactions are lost, and the material begins to precipitate. This loss of stability is further aggravated by the increase in ionic strength in PBS (Echeverri-Cuartas *et al.*, 2020). Additionally, the glacial acetic acid remaining in scaffolds could be for the 1% Ch synthesis and, this indicates that the scaffolds must be washed to remove it with PBS before the cell culture.

### *3.5. Matrixes Biological Effect*

Taking into account that Alg/Ch scaffolds were crosslinked with GEN and functionalized with VEGF-A, that scaffolds have interconnected pores, with different sizes of diameters (between 1 to 280 μm), suitable ranges for β cells and pancreatic islets, the effect of scaffolds M1 to M5 on the viability and proliferation of insulin-producing cells was evaluated in order to determine if the scaffolds produce a microenvironment that favours the survival and proliferation of β pancreatic cells.

In this line, Figure 6a shows that, all concentrations maintain cell viability at different levels respect to the control cells. Specifically, the graph shows that scaffolds M4 and M5 functionalized with VEGF-A maintain better cell viability (121 % and 148 %, respectively) upper 80% in contrast with the scaffolds M1 (62.2 %), M2 (65.3 %) and M3 (73.9 %).

Additionally, the LDH assay (Figure 6b) shows the lowest release of LDH to the media with the scaffolds M4 and M5 functionalized with VEGF-A (29.2 % and 20.5 %, respectively). This result suggests the lowest percentage of membrane β cell rupture with VEGF-A scaffolds in contrast with the scaffolds M1 (52.9 %), M2 (41.8 %) and M3 (30.2 %) and a high cytotoxic effect of the M1, M2 and M3 samples compared to the control of dead cells. Those results are confirmed by the live and dead technique where the same proportions of live and dead cells could be visualized in each condition (Figure 6c).


Revista EIA | https://doi.org/10.24050/reia.v22i43.1838

**Figure 6.** Beta pancreatic cell viability and proliferation on Alg/Ch/GEN functionalized scaffolds. (a) MTT assay as percentage of viable cells on M1 to M5 samples. (b) lactate dehydrogenase (LDH) release study. (c) Live/dead staining of pancreatic cells on plate (control) and M1 to M5 samples cell culture. (Green = FDA (live); red = PI (dead)); scale bar = 100 µm. (d) PicoGreen assay results showing total DNA content of cells on plate cell culture, M1 to M5 samples cultured. " *, **, *** " denotes a statistically significant difference ($p < 0.05$) in cell number with respect to the culture plate cells (TCP). Data points represent mean ± SD (n = 3).

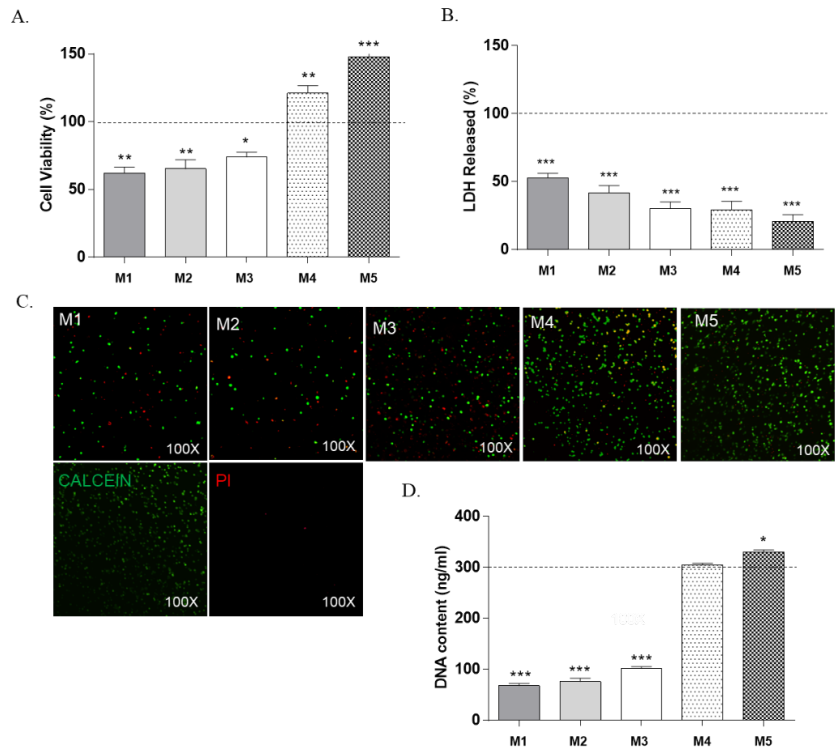


The evaluation of cytotoxicity using MTT was in accordance with the ISO2109932-5 standard, using a 5-point grading scale, as was described before (Li *et al.*, 2016). Specifically, VEGF-A maintains better cell viability -upper 80% suggesting a cell growth relative rate grade 0, suggesting no cytotoxicity (Li *et al.*, 2016). However, samples M1, M2 and M3 samples according to the scale show a Grade 2 and represent mild cytotoxicity (Li *et al.*, 2016). All these results were confirmed with cytotoxic effects with LDH. To note, the beta pancreatic cell viability was improved with the GEN addition to the scaffold with respect to M1 (without GEN), and a better cell viability dependent of GEN concentration was identified. In this sense, it could be due that GEN could inhibit the uncoupling protein 2 (UCP2-a protein associated with diabetes development)

(Zhang et al., 2001; Zhang et al., 2006) such as GEN promotes the passage of electrons across the mitochondrial membrane, helping to trigger the electron transport chain, it ultimately promotes ATP production in pancreatic cells (Zhang *et al.*, 2001, 2006) and GEN has been shown to even increase the insulin secretion of insulin after high glucose treatments on islets explants (Parton *et al.*, 2007; Zhang *et al.*, 2006), all those positive effects on beta cells could explain better cell viability improved with the most higher GEN concentration used in the scaffold development. However, only high GEN concentrations were not enough to reduce the cytotoxicity grade on beta cells as shown in our MTT, live and dead and LDH results. Nevertheless, only after VEGF-A addition the beta cell viability was improved to a grade 0 or no toxic effect of the biomaterial. This could be explained since VEGF-A promotes cell survival (Lammert *et al.*, 2003; Phelps *et al.*, 2015; Zhang *et al.*, 2004) and even was described as a VEGF-A protection against beta cell death due mainly to the hypervascularisation of the biomaterial (De Leu *et al.*, 2014).

All these results not only confirm the cell viability results, but also suggest that there is a joint work effect with the treatment of GEN and VEGF-A samples to preserve the integrity of the pancreatic beta cell membrane and maintain the cell viability of pancreatic cells.

Finally, the proliferation of insulin-producing cells was evaluated. Figure 6d show a significant increase in proliferation of β cells with scaffold M5 (330.5 %) with respect to the control. This result could be due to the GEN percentage (1%) [40] and VEGF-A functionalization (De Leu *et al.*, 2014). The VEGF-A effect on beta proliferation was described before in vivo and in vitro assays, showing that induces a process of beta cell regeneration and cell proliferation studies (Lammert *et al.*, 2003; De Leu *et al.*, 2014; Staels *et al.*, 2019).

The findings made show the usefulness of the Alg/Ch GEN 1% scaffold functionalized with VEGF-A as a biodegradable, biocompatible, low toxicity, relatively low-cost scaffold with a similar structure to the microenvironment of the beta pancreatic cell, which preserves the viability and favours the proliferation of beta cells, this, in turn, could represent an advantage improving the functionality of the pancreatic beta-cell, vascularization after transplantation and reduction of rejection when implanted in the body human as a


Revista EIA https://doi.org/10.24050/reia.v22i43.1838

screening for the diabetes treatment. Future studies could focus on the effect of the scaffolds designed on the beta cell functionality and animal transplantation.

## 4. Conclusions

In conclusion, our work shows the application of a scaffold of Alg/Ch crosslinking with GEN 1% and functionalized with VEGF-A by the chemical crosslinking method. The designed scaffold has an appropriate pore size for the diffusion of nutrients necessary for pancreatic cells (200 μm), they are scaffolds that retain their structure for long periods of time, absorb nutrients in a stable manner, in turn, favour protection against cell death-inducing an appropriate environment to preserve viability and even by the action of VEGF-A in combination with GEN 1%, induces the proliferation of beta cells.

## 5. Data Availability

The data that support the findings of this study are available from the corresponding author upon reasonable request.

## 6. Conflicts of Interest

The authors declare no competing financial interest. All authors have read and agree to the published version of the manuscript.

## 7. Funding Statement

This research was supported by Ministerio de Ciencia, Tecnología e innovación de Colombia-Minciencias code: 110284466876 announcement 844-2019. Universidad Industrial de Santander. Universidad EIA. Hospital Pablo Tobón Uribe. Vicerrectoría de investigación y extension, Universidad Industrial de Santander-international mobility program for professors.

## 8. Acknowledgments

The authors thank Raquel E. Ocazionez for the infrastructure support. Graphical abstract was created with BioRender.com. Data curation, Formal analysis and Methodology, M.B.R., C.E.E.-C., M.E.L.L., and N.M.-C.; Funding acquisition and project administration, N.M.-C. Writing—original draft, MBR, C.E.E.-C., MELL and N.M.-C.

## 9. Ethical approval

The ethics committee from the University Industrial de Santander approved this study (code: 4110) on 10 May 2019.

## References

Anjani, Q.K., Sabri, A.H. Bin, Moreno-Castellanos, N., Utomo, E., Cárcamo-Martínez, Á., Domínguez-Robles, J., Wardoyo, L.A.H., *et al.* (2022), "Soluplus®-based dissolving microarray patches loaded with colchicine: towards a minimally invasive treatment and management of gout", *Biomaterials Science*, Biomater Sci, Vol. 10 No. 20, pp. 5838–5855, doi: 10.1039/D2BM01068B.

Antonova, L. V., Sevostyanova, V. V., Kutikhin, A.G., Mironov, A. V., Krivkina, E.O., Shabaev, A.R., Matveeva, V.G., *et al.* (2016), "Vascular Endothelial Growth Factor Improves Physico-Mechanical Properties and Enhances Endothelialization of Poly(3-hydroxybutyrate-co-3-hydroxyvalerate)/Poly(ε-caprolactone) Small-Diameter Vascular Grafts In vivo", *Frontiers in Pharmacology*, Front Pharmacol, Vol. 7 No. JUL, doi: 10.3389/FPHAR.2016.00230.

Belén, L., Yalli, F., Pastor De Abram, A. and Fuentes Yalli, L. (2009), "PREPARACIÓN, CARACTERIZACIÓN Y EVALUACIÓN DE PELÍCULAS DE QUITOSANO PROVENIENTE DE CALAMAR GIGANTE " PARA USO MÉDICO PREPARATION, CHARACTERIZATION AND CHITOSAN FILMS EVALUATION FROM GIANT SQUID " ' FOR MEDICAL USE Dosidicus gigas' Dosidicus gigas", *Rev Soc Quím Perú*, Vol. 75 No. 1.

Bertram, R. and Pernarowski, M. (1998), "Glucose diffusion in pancreatic islets of Langerhans", *Biophysical Journal*, Biophys J, Vol. 74 No. 4, pp. 1722–1731, doi: 10.1016/S0006-3495(98)77883-X.

Brawerman, G. and Thompson, P.J. (2020), "Beta Cell Therapies for Preventing Type 1 Diabetes: From Bench to Bedside", *Biomolecules*, Biomolecules, Vol. 10 No. 12, pp. 1–20, doi: 10.3390/BIOM10121681.

Chakka, J.L., Acri, T., Laird, N.Z., Zhong, L., Shin, K., Elangovan, S. and Salem, A.K. (2021), "Polydopamine functionalized VEGF gene-activated 3D printed scaffolds for bone regeneration", *RSC Advances*, RSC Adv, Vol. 11 No. 22, pp. 13282–13291, doi: 10.1039/D1RA01193F.

Chua, S.T., Song, X. and Li, J. (2018), "Hydrogels for Stem Cell Encapsulation: Toward Cellular Therapy for Diabetes", *Springer Series in Biomaterials Science and Engineering*, Springer, Berlin, Heidelberg, Vol. 12, pp. 113–127, doi: 10.1007/978-3-662-57511-6_5.

Dhamecha, D., Movsas, R., Sano, U. and Menon, J.U. (2019), "Applications of alginate microspheres in therapeutics delivery and cell culture: Past, present and future", *International Journal of Pharmaceutics*, Int J Pharm, Vol. 569, doi: 10.1016/J.IJPHARM.2019.118627.

Dimida, S., Barca, A., Cancelli, N., De Benedictis, V., Raucci, M.G. and Demitri, C. (2017), "Effects of genipin concentration on cross-linked chitosan scaffolds for bone tissue engineering: Structural characterization and evidence of biocompatibility features", *International Journal of Polymer Science*, Hindawi Limited, Vol. 2017, doi: 10.1155/2017/8410750.

Echeverri-Cuartas, C.E., Gartner, C. and Lapitsky, Y. (2020), "PEGylation and folate conjugation effects on the stability of chitosan-tripolyphosphate nanoparticles", *International Journal of Biological Macromolecules*, Int J Biol Macromol, Vol. 158, pp. 1055–1062, doi: 10.1016/J.IJBIOMAC.2020.04.118.

Gao, L., Gan, H., Meng, Z., Gu, R., Wu, Z., Zhang, L., Zhu, X., *et al.* (2014), "Effects of genipin cross-linking of chitosan hydrogels on cellular adhesion and viability", *Colloids and Surfaces. B, Biointerfaces*, Colloids Surf B Biointerfaces, Vol. 117, pp. 398–405, doi: 10.1016/J.COLSURFB.2014.03.002.

Garnica-Palafox, I.M., Estrella-Monroy, H.O., Vázquez-Torres, N.A., Álvarez-Camacho, M., Castell-Rodríguez, A.E. and Sánchez-Arévalo, F.M. (2020), "Influence of multi-walled carbon nanotubes on the physico-chemical and biological responses of chitosan-based hybrid hydrogels", *Carbohydrate Polymers*, Elsevier, Vol. 236, p. 115971, doi: 10.1016/J.CARBPOL.2020.115971.

Hommel, J., Coltman, E. and Class, H. (2018), "Porosity–Permeability Relations for Evolving Pore Space: A Review with a Focus on (Bio-)geochemically Altered Porous Media", *Transport in Porous Media*, Springer Netherlands, Vol. 124 No. 2, pp. 589–629, doi: 10.1007/S11242-018-1086-2/FIGURES/1.

Hsieh, W.C., Chang, C.P. and Lin, S.M. (2007), "Morphology and characterization of 3D micro-porous structured chitosan scaffolds for tissue engineering", *Colloids and Surfaces. B, Biointerfaces*, Colloids Surf B Biointerfaces, Vol. 57 No. 2, pp. 250–255, doi: 10.1016/J.COLSURFB.2007.02.004.

Hu, S. and de Vos, P. (2019), "Polymeric Approaches to Reduce Tissue Responses Against Devices Applied for Islet-Cell Encapsulation", *Frontiers in Bioengineering and Biotechnology*, Front Bioeng Biotechnol, Vol. 7, doi: 10.3389/FBIOE.2019.00134.

Ichihara, Y., Utoh, R., Yamada, M., Shimizu, T. and Uchigata, Y. (2016), "Size effect of engineered islets prepared using microfabricated wells on islet cell function and arrangement", *Heliyon*, Heliyon, Vol. 2 No. 6, doi: 10.1016/J.HELIYON.2016.E00129.

Kildeeva, N., Chalykh, A., Belokon, M., Petrova, T., Matveev, V., Svidchenko, E., Surin, N., *et al.* (2020), "Influence of Genipin Crosslinking on the Properties of Chitosan-Based Films", *Polymers*, Polymers (Basel), Vol. 12 No. 5, doi: 10.3390/POLYM12051086.

Klein, M.P., Hackenhaar, C.R., Lorenzoni, A.S.G., Rodrigues, R.C., Costa, T.M.H., Ninow, J.L. and Hertz, P.F. (2016), "Chitosan crosslinked with genipin as support matrix for application in food process: Support characterization and β-D-galactosidase immobilization", *Carbohydrate Polymers*, Carbohydr Polym, Vol. 137, pp. 184–190, doi: 10.1016/J.CARBPOL.2015.10.069.

Lammert, E., Gu, G., McLaughlin, M., Brown, D., Brekken, R., Murtaugh, L.C., Gerber, H.P., *et al.* (2003), "Role of VEGF-A in vascularization of pancreatic islets", *Current Biology : CB*, Curr Biol, Vol. 13 No. 12, pp. 1070–1074, doi: 10.1016/S0960-9822(03)00378-6.

De Leu, N., Heremans, Y., Coppens, V., Van Gassen, N., Cai, Y., D'Hoker, J., Magenheim, J., *et al.* (2014), "Short-term overexpression of VEGF-A in mouse beta cells indirectly stimulates their proliferation and protects against diabetes", *Diabetologia*, Springer, Vol. 57 No. 1, pp. 140–147, doi: 10.1007/S00125-013-3076-9/FIGURES/5.

Li, B.-B., Yin, Y.-X., Yan, Q.-J., Wang, X.-Y. and Li, S.-P. (2016), "A novel bioactive nerve conduit for the repair of peripheral nerve injury.", *Neural Regeneration Research*, Editorial Board of Neural Regeneration Research, Vol. 11 No. 1, pp. 150–5, doi: 10.4103/1673-5374.175062.

Madden, L.R., Mortisen, D.J., Sussman, E.M., Dupras, S.K., Fugate, J.A., Cuy, J.L., Hauch, K.D., *et al.* (2010), "Proangiogenic scaffolds as functional templates for cardiac tissue engineering", *Proceedings of the National Academy of Sciences of the United States of America*, National Academy of Sciences, Vol. 107 No. 34, pp. 15211–15216, doi: 10.1073/PNAS.1006442107/-/DCSUPPLEMENTAL.

Maji, K., Dasgupta, S., Pramanik, K. and Bissoyi, A. (2016), "Preparation and Evaluation of Gelatin-Chitosan-Nanobioglass 3D Porous Scaffold for Bone Tissue Engineering", *International Journal of Biomaterials*, Int J Biomater, Vol. 2016, doi: 10.1155/2016/9825659.

Maniruzzaman, M., Rahman, M.J., Ahammed, B. and Abedin, M.M. (2020), "Classification and prediction of diabetes disease using machine learning paradigm", *Health Information Science and Systems*, Health Inf Sci Syst, Vol. 8 No. 1, doi: 10.1007/S13755-019-0095-Z.

Nishiyama, N. and Yokoyama, T. (2017), "Permeability of porous media: Role of the critical pore size", *Journal of Geophysical Research: Solid Earth*, Blackwell Publishing Ltd, Vol. 122 No. 9, pp. 6955–6971, doi: 10.1002/2016JB013793.

Norris, J.M., Johnson, R.K. and Stene, L.C. (2020), "Type 1 diabetes-early life origins and changing epidemiology", *The Lancet. Diabetes & Endocrinology*, Lancet Diabetes Endocrinol, Vol. 8 No. 3, pp. 226–238, doi: 10.1016/S2213-8587(19)30412-7.

Parton, L.E., Ye, C.P., Coppari, R., Enriori, P.J., Choi, B., Zhang, C.Y., Xu, C., *et al.* (2007), "Glucose sensing by POMC neurons regulates glucose homeostasis and is impaired in obesity", *Nature*, Nature, Vol. 449 No. 7159, pp. 228–232, doi: 10.1038/NATURE06098.

Phelps, E.A., Templeman, K.L., Thulé, P.M. and García, A.J. (2015), "Engineered VEGF-releasing PEG-MAL hydrogel for pancreatic islet vascularization", *Drug Delivery and Translational Research*, Drug Deliv Transl Res, Vol. 5 No. 2, pp. 125–136, doi: 10.1007/S13346-013-0142-2.

Queiroz, M.F., Melo, K.R.T., Sabry, D.A., Sassaki, G.L. and Rocha, H.A.O. (2015), "Does the Use of Chitosan Contribute to Oxalate Kidney Stone Formation?", *Marine Drugs*, Multidisciplinary Digital Publishing Institute (MDPI), Vol. 13 No. 1, p. 141, doi: 10.3390/MD13010141.

Sánchez-Cardona, Y., Echeverri-Cuartas, C.E., López, M.E.L. and Moreno-Castellanos, N. (2021), "Chitosan/Gelatin/PVA Scaffolds for Beta Pancreatic Cell Culture", *Polymers*, Polymers (Basel), Vol. 13 No. 14, doi: 10.3390/POLYM13142372.

Shi, G., Cai, Q., Wang, C., Lu, N., Wang, S. and Bei, J. (2002), "Fabrication and biocompatibility of cell scaffolds of poly(L-lactic acid) and poly(L-lactic-co-glycolic acid)", *Polymers for Advanced Technologies*, John Wiley & Sons, Ltd, Vol. 13 No. 3–4, pp. 227–232, doi: 10.1002/PAT.178.

Song, S. and Roy, S. (2016), "Progress and challenges in macroencapsulation approaches for type 1 diabetes (T1D) treatment: Cells, biomaterials, and devices", *Biotechnology and Bioengineering*, Biotechnol Bioeng, Vol. 113 No. 7, pp. 1381–1402, doi: 10.1002/BIT.25895.

Staels, W., Heremans, Y., Heimberg, H. and De Leu, N. (2019), "VEGF-A and blood vessels: a beta cell perspective", *Diabetologia*, Diabetologia, Vol. 62 No. 11, pp. 1961–1968, doi: 10.1007/S00125-019-4969-Z.

Tavares, L., Esparza Flores, E.E., Rodrigues, R.C., Hertz, P.F. and Noreña, C.P.Z. (2020), "Effect of deacetylation degree of chitosan on rheological properties and physical chemical characteristics of genipin-crosslinked chitosan beads", *Food Hydrocolloids*, Elsevier, Vol. 106, p. 105876, doi: 10.1016/J.FOODHYD.2020.105876.

Yang, K., O'Cearbhaill, E.D., Liu, S.S., Zhou, A., Chitnis, G.D., Hamilos, A.E., Xu, J., *et al.* (2021), "A therapeutic convection-enhanced macroencapsulation device for enhancing β cell viability and insulin secretion", *Proceedings of the National Academy of Sciences of the United States of America*, Proc Natl Acad Sci U S A, Vol. 118 No. 37, p. 1DUMMUY, doi: 10.1073/PNAS.2101258118.

Zhang, C.Y., Baffy, G., Perret, P., Krauss, S., Peroni, O., Grujic, D., Hagen, T., *et al.* (2001), "Uncoupling protein-2 negatively regulates insulin secretion and is a major link between obesity, beta cell dysfunction, and type 2 diabetes", *Cell*, Cell, Vol. 105 No. 6, pp. 745–755, doi: 10.1016/S0092-8674(01)00378-6.

Zhang, C.Y., Parton, L.E., Ye, C.P., Krauss, S., Shen, R., Lin, C.T., Porco, J.A., *et al.* (2006), "Genipin inhibits UCP2-mediated proton leak and acutely reverses obesity- and high glucose-induced β cell dysfunction in isolated pancreatic islets", *Cell Metabolism*, Cell Press, Vol. 3 No. 6, pp. 417–427, doi: 10.1016/J.CMET.2006.04.010.

Zhang, L., Vincent, M.A., Richards, S.M., Clerk, L.H., Rattigan, S., Clark, M.G. and Barrett, E.J. (2004), "Insulin sensitivity of muscle capillary recruitment in vivo", *Diabetes*, Diabetes, Vol. 53 No. 2, pp. 447–453, doi: 10.2337/DIABETES.53.2.447.

Zhao, D., Yu, S., Sun, B., Gao, S., Guo, S. and Zhao, K. (2018), "Biomedical Applications of Chitosan and Its Derivative Nanoparticles", *Polymers*, Multidisciplinary Digital Publishing Institute (MDPI), Vol. 10 No. 4, doi: 10.3390/POLYM10040462.